# ARTICLES

## Exploring the Time-Scales of H-Atom Detachment from Photoexcited Phenol-$h_6$ and Phenol-$d_5$: Statistical vs Nonstatistical Decay

**Azhar Iqbal,[†] Michelle S. Y. Cheung,[†] Michael G. D. Nix,[‡] and Vasilios G. Stavros*,[†]**

*Department of Chemistry, University of Warwick, Coventry CV4 7AL, U.K., and School of Chemistry, University of Bristol, Bristol BS8 1TS, U.K.*

*Received: April 4, 2009; Revised Manuscript Received: May 19, 2009*

The prevalence of $^1\pi\sigma^*$ states in the photochemistry of heteroaromatics is becoming increasingly clear from the recent literature. Photodissociation measurements have shown that following excitation of phenol molecules above the $S_1/S_2$ conical intersection, H-atoms are eliminated with two distinct ranges of kinetic energy release. Those with high kinetic energy are attributed to direct dissociation while those with low kinetic energy are traditionally attributed to indirect dissociation or statistical unimolecular decay, both pathways giving electronic ground-state phenoxyl fragments. Using a combination of femtosecond pump/probe spectroscopy and velocity map ion imaging techniques, the time and energy resolved H-atom elimination in phenol-$h_6$ and phenol-$d_5$, following excitation at 200 nm has been measured. At the lowest kinetic energies, the H-atom elimination from phenol-d5 occurs in <150 fs, in sharp contrast to what one expects from a statistical decay process. This implies that these H-atoms are formed through a direct dissociation process yielding electronically excited phenoxyl fragments.

## Introduction

Ab initio calculations by Sobolewski and Domcke[1] have fuelled a great deal of interest in the photofragmentation[2] of various biomolecules and their prototypical chromophores. The potential energy surfaces (PES) of these molecules contain a singlet $^1\pi\sigma^*$ state that is repulsive with respect to the X—H coordinate (where X is the heteroatom, typically N or O). The repulsive character of this electronic state gives rise to nonradiative decay in these molecules following absorption of UV radiation. The nonradiative processes may impart photostability, protecting these molecules from dangerous photoinduced reactions.[3,4]

Phenol, the chromophore of the amino acid tyrosine, has been a prime focus in recent years, being a prototype molecule for developing a better understanding of electronic structure and photochemistry of other, larger heteroaromatic biomolecules. Sobolewski, Domcke, and co-workers[5−7] have shown that the low fluorescence quantum yield of phenol following excitation at the wavelength of interest here (200 nm) is primarily due to an excited singlet state of $^1\pi\sigma^*$ ($S_2$) character, which is dissociative with respect to the stretching coordinate of the O—H bond. This dissociative state ($S_2$) lies below the upper $^1\pi\pi^*$ ($S_3$) state but intersects both the optically bright $^1\pi\pi^*$ state ($S_1$) and the ground state ($S_0$) through two successive conical intersections (CI, $S_1/S_2$, and $S_0/S_2$, respectively), leading to elimination of neutral hydrogen (see Figure 1a in Ashfold et al.[8]). Due to the weak $S_2 \leftarrow S_0$ transition, $S_2$ is not excited directly and is populated by radiationless transfer from the optically bright $S_1$

state or, at these higher energies, from another $^1\pi\pi^*$ ($S_3$) state that dominates the absorption when $\lambda$ < 220 nm.[2,9] Following population of the $S_2$ state, the excited phenol molecule evolves toward the $S_0/S_2$ CI with two possible photochemical fates. The molecule can eliminate an H atom from the heteroatom site directly via the repulsive $^1\pi\sigma^*$ state or, alternatively, highly excited ground-state phenol molecules may be formed which can also release H atoms when sufficient energy becomes localized in the correct vibrational mode following intramolecular vibrational relaxation (IVR). These H-atom elimination pathways are commonly referred to as direct dissociation and statistical unimolecular decay respectively.[8]

The ability to disentangle the contributions from the direct and statistical pathways to dissociation of these hydrides (X—H) is of considerable value as this can provide detailed information about the nature of the coupling of PES at the various CIs. This paper describes the application of time-resolved velocity map ion imaging (TRVMI) which enables one to clock the real-time H-atom elimination with energy dependence and thus establish a time constant for dissociation via the different pathways. Direct dissociation is known to yield H-atoms with large amounts of kinetic energy, due to the repulsive nature of the $^1\pi\sigma^*$ state, while indirect dissociation typically leads to H-atoms with much less kinetic energy on average. Disentangling these two pathways is possible as VMI enables one to separate H-atoms with varying amounts of kinetic energy within the image. The work described herein shows that both high and low kinetic energy H-atoms are released on an ultrafast (<150 fs) time scale, in sharp contrast to what one would expect via an IVR mediated statistical pathway for the low kinetic energy H-atoms. This casts considerable doubt over the previously assigned statistical pathway for dissociation yielding these H-atoms, as determined

* Author to whom correspondence should be addressed. E-mail: v.stavros@warwick.ac.uk.
† University of Warwick.
‡ University of Bristol.

through multimass ion-imaging and total kinetic energy release measurements.

The H-atom elimination through the $S_2$ state was first reported by Tseng et al.[10–12] using multimass ion-imaging. Following excitation at 248 and 193 nm, the H-detachment from photo-excited phenol-$h_6$ molecules occurred through two channels: One channel gave high kinetic energy H-atoms attributed to direct coupling of the $^1\pi\pi*$ with the $^1\pi\sigma*$ state at the $S_1/S_2$ CI, and the $S_0/S_2$ CI;[10] The second channel resulted in low kinetic energy H-atoms, which were assumed to be formed from internal conversion to the ground state, followed by dissociation. As the excitation energy increased, the proportion of low kinetic energy H-atoms increased, apparently due to the increasing rate of internal conversion.[12] This argument was to some extent supported by the recent calculations of Vieuxmaire et al.[13] which identified a prefulvenic conical intersection ($CI_{pref}$) existing at excitation energies of about 2300 cm$^{-1}$ above the $S_1/S_2$ CI. At these energies, the prefulvenic decay channel opens, providing a direct nonradiative passage from the photoexcited $^1\pi\pi*$ state through $CI_{pref}$ to the $S_0$ PES. This channel should compete with the direct H-atom detachment process, thus enhancing the formation of highly vibrationally excited $S_0$ molecules which undergo IVR mediated H-atom elimination on the ground-state $S_0$.

Following excitation above the $S_1/S_2$ CI, the total kinetic energy release (TKER) measurements by Nix et al.[8,2] reported two primary peaks in the H-atom TKER spectrum. They attributed the peak corresponding to the highest kinetic energy ($\sim$12 000 cm$^{-1}$) to direct dissociation while the low-energy peak was assigned as being due to statistical unimolecular decay of very highly excited phenol-$h_6$ ($S_0$) molecules such as those formed due to coupling at the $S_0/S_2$ or prefulvenic CIs, following single or multiphoton excitation. The observed TKE $R_{max}$ of this statistical channel was too high to originate from purely single photon processes. In more recent measurements using velocity map ion imaging (VMI), Hause et al.[14] also attributed the intensity of the H$^+$ signal in the center of their ion image, i.e., H-atoms with low kinetic energy, to statistical internal conversion and multiphoton dissociation.

The importance of statistical deactivation following UV absorption is an area of growing interest,[15] as exemplified by the recent work in cationic amino acid dipeptides such as tryptophan−leucine.[16] Understanding the role of this pathway from the smallest subunit, the chromophore, would assist us in understanding the photophysics of much larger systems such as dipeptides and polypeptides. As shown by the groups of Ashfold, Ni, and Crim, the low kinetic energy H-atoms observed in their measurements often point toward a statistical deactivation pathway. Their argument is further strengthened by the observed isotropic nature of the H-atom photofragment distribution, wherein the measured anisotropy parameter $\beta_2 \approx 0$, suggesting dissociation on a long time scale relative to molecular rotation.

The ability to measure directly the time scales of both high and low kinetic energy H-atom release provides detailed insight into the dynamics of these two decay channels and therefore represents a step forward in aiding our understanding of statistical vs non statistical decay dynamics in some of nature's most important photoactive molecules. To the best of our knowledge, the only time-resolved H-atom detachment demonstrations in such heteroaromatic chromophores have been achieved by Lippert et al.[17] in pyrrole and more recently by our group in phenol.[18] In this latter work, we reported that, following excitation at 200 nm and probing the neutral H atoms

via (2 + 1) resonance enhanced multiphoton ionization (REMPI) at 243.1 nm, H atom elimination from photoexcited phenol molecules occurred within $103 \pm 30$ fs. This we attributed to the very efficient coupling of PESs at the $S_1/S_2$ and $S_0/S_2$ CIs, with no identifiable role of statistical unimolecular decay on the time scale of our measurements (<200 ps). However, both our work and the work of Lippert et al.[17] measured the total H$^+$ signal. The current work uses a combination of pump/probe spectroscopy and VMI, which enables us to clock the real-time dissociation of H-atom elimination with both time *and* energy resolution. The extra dimension afforded by VMI means that we are now able to measure the appearance times for both the fast (high kinetic energy) and slow (low kinetic energy) H-atoms. The measured appearance time of the slow H-atoms (<150 fs), casts doubt over their origin as being from a statistical process, implying that they are more likely formed through a direct pathway.

This paper attempts to pinpoint the various H-atom elimination pathways in photoexcited phenol-$h_6$ ($C_6H_5$−OH) and phenol-$d_5$ ($C_6D_5$−OH) molecules. The purpose of studying phenol-$d_5$ is to eliminate the contribution, if any, of H from the phenyl ring. We present energy *and* time-resolved H$^+$ transients originating from both phenol-$h_6$ and phenol-$d_5$, discussing their origin in terms of the known or proposed dynamics of dissociation. The results of these findings are summarized and the consequences of these findings briefly discussed with reference to other biologically relevant hydrides that have been suggested to exhibit similar decay dynamics.

## Experimental Section

The experiment has been described in detail elsewhere,[18,19] and only a brief description is given here. The optical setup uses a commercial femtosecond laser system (Spectra-Physics XP) containing a Ti-sapphire oscillator and a regenerative amplifier. The system operates at 1 kHz, generating 3 mJ, 35 fs pulses centered at 800 nm. The fundamental output is split into three beams of equal intensity. To generate the fourth harmonic, 1 mJ/pulse is sent through a series of nonlinear type I and type II BBO ($\beta$-barium borate) crystals resulting in pump pulses of approximately 1 $\mu$J/pulse at 200 nm by frequency doubling the 800 nm and then combining the 400 nm radiation with residual 800 nm radiation in two mixing stages. The remaining two beams are used to pump two optical parametric amplifiers (TOPAS model 4/800/f, Light Conversion). Only one is used in these measurements, whose output power is around 6−7 $\mu$J/pulse, set at 243.1 nm to probe neutral H atoms via (2 + 1) REMPI. The pump and probe pulses are combined collinearly with the help of a dichroic mirror and focused with the aid of a 500 mm magnesium fluoride lens into the interaction region of a VMI spectrometer, intercepting a molecular beam of phenol. The instrument response function has a measured full-width half-maximum (fwhm) of 160 fs. The relative delay between the pump and probe is controlled by a delay stage (Physik-Instrumente), the probe being typically varied over 3 ps with a minimum step size of 0.025 ps. A molecular beam of phenol-$h_6$ (Fluka, $\geq$ 99.5%) or phenol-$d_5$ (Sigma-Aldrich, phenol-2,3,4,5,6-$d_5$, 98 atom % D) is produced by seeding a vapor pressure of the target molecule in He (2−3 psi and 70 °C) which is admitted into the vacuum using an Even-Lavie pulsed solenoid valve[20] operating at 500 Hz and synchronized to the laser system. The source chamber houses the pulsed-valve, the molecular beam passing through a 2 mm skimmer separating the source chamber from the interaction chamber. The interaction chamber contains the VMI detector, replicating

the setup as described by Eppink and Parker,[21] to detect H-atoms. The ion optics comprise a repeller, extractor, and ground electrodes. The $H^+$ ions are extracted toward the detector consisting of a 40 mm diameter Chevron microchannel plate (MCP) assembly coupled to a P-43 phosphor screen (Photek). By applying a timed voltage pulse (Behlke) on the second MCP, we gate on a particular mass ion (in this case $H^+$) and record the 2-D images as described in our previous paper.[19] The deconvolution of the raw images is done by using an acquisition program written in LABVIEW which uses the polar onion peeling method.[22]

## Results and Discussion

Figure 1a,b shows raw images of $H^+$ obtained by dissociating phenol-$h_6$ and phenol-$d_5$, respectively, following excitation at 200 nm and probing with 243.1 nm radiation. Only half of each image is shown for illustrative purposes, separated by the horizontal dashed line, each image having been cut centrally along the axis perpendicular to the laser polarization (bold double arrow). The delay between the pump and probe pulses (*t*) was set to 2 ps. Both images look qualitatively very similar, with an intense central region and a sharper outer ring. The outer ring arises from ionization of kinetically energetic neutral H-atoms formed via direct dissociation through both the $S_1/S_2$ and $S_0/S_2$ CIs and most likely another, as yet uncharacterized $S_2/S_3$ CI, yielding fast H-atoms and ground-state phenoxyl cofragments. The outer ring corresponds to H-atoms with kinetic energies of approximately 11 600 $cm^{-1}$ and clearly displays anisotropy, with a measured anisotropy parameter of $\beta_2 \approx 0.4$, implying a greater contribution of dissociation parallel to the polarization axis of the laser beam. The ions in the center of the image originate as H-atoms that are born with very low kinetic energy, and on the basis of the current arguments given in the literature, we would anticipate them to be largely a result of some statistical decay process. Immediately apparent, however, is that the centralized spot occurs even at a 2 ps time delay between pump and probe pulses. It is important to stress here that, first, when the probe pulse precedes the pump pulse, there is negligible $H^+$ signal, indicating that this signal is truly two-color and, second, detuning the TOPAS output from the $2s \leftarrow 1s$ resonance in H considerably reduces the $H^+$ signal in phenol-$d_5$, indicating that the $H^+$ detected are indeed neutral H-atoms from dissociation of O—H, which are being probed, rather than nascent $H^+$ ions originating from multiphoton ion fragmentation channels. Both these observations will be discussed and rationalized in further detail in the proceeding discussion.

Parts a and b of Figure 2 show the transient $H^+$ as a function of kinetic energy for two pump/probe delays for phenol-$h_6$ and phenol-$d_5$, respectively. When the pump is preceded by the probe, there is no $H^+$ signal present and, these data are therefore not shown. At $t = 0$, where *t* refers to the delay
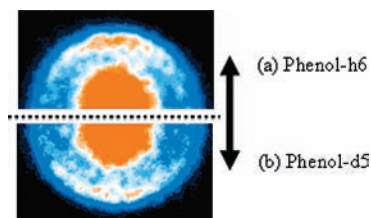


**Figure 1.** Raw images for $H^+$ following photodissociation at 200 nm and probing with 243.1 nm. Only half of each image is shown for illustrative purposes for (a) phenol-$h_6$ and (b) phenol-$d_5$, respectively. In both figures, the 243.1 nm probe was preceded by the pump by a delay of 2 ps.
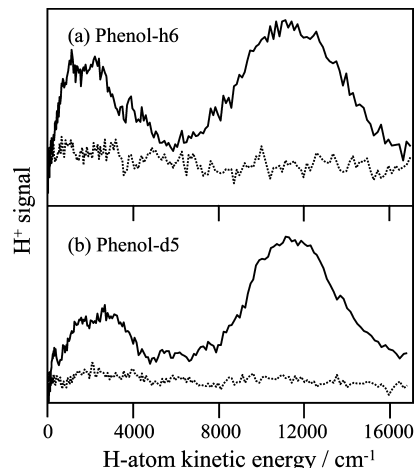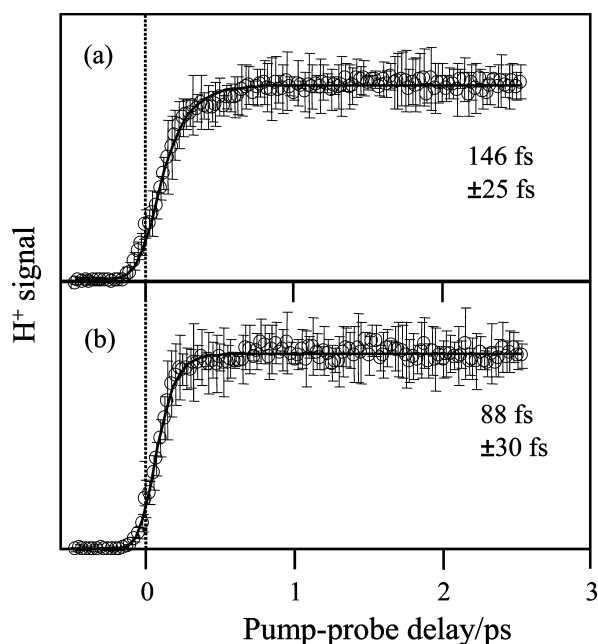


**Figure 2.** $H^+$ transient as a function of H-atom kinetic energy (dashed and solid lines correspond to pump/probe delays (*t*) of 0 and 2 ps, respectively) for (a) phenol-$h_6$ and (b) phenol-$d_5$ molecules. At $t < 0$ there is no appreciable $H^+$ signal and therefore these transients are excluded for clarity.

between the pump and probe pulses, i.e., when the pump and probe are temporally overlapped, the $H^+$ signal appears (dashed line). The signal grows with increasing *t*, but the kinetic energy spectrum remains unchanged from 500 fs onward and a representative example is shown by the solid line, corresponding to a 2 ps pump/probe delay. As is evident from both figures, there are two distinct peaks in the spectra, with maxima occurring at approximately 11 600 $cm^{-1}$ for fast H-atoms and at 2700 $cm^{-1}$ for slow H-atoms. The shape of these kinetic energy distributions is in very good agreement with those obtained for nanosecond single photon dissociation by Ashfold et al.[8] and more recently by Hause et al.[14]

Deuterating the C—H bonds in phenol and probing for H-atoms removes any contribution to the signal from the H-atoms of the phenyl ring. As is evident in Figure 2a,b, the peak intensity of the low kinetic energy H-atoms in phenol-$d_5$ is somewhat less than that of the high kinetic energy H-atoms (Figure 2b) whereas the peak intensity of the low kinetic energy H-atoms in phenol-$h_6$ is comparable to that of the high kinetic energy H-atoms (Figure 2a). This illustrates some contribution of phenyl ring C—H fission to the signal in phenol-$h_6$, as observed by Hause et al.[14] Multiphoton effects are likely candidates for generating $H^+$ directly from any H atom site. This is quite clearly illustrated in Figure 3a,b. Once again, these figures show the transient $H^+$ as a function of kinetic energy at a pump/probe delay of 2 ps. The solid and dashed lines correspond to the probe pulse centered at 243.1 and 238 nm, respectively. When the probe wavelength is detuned from the H atom $2s \leftarrow 1s$ resonance using 238 nm radiation, the $H^+$ signal is reduced considerably in phenol-$d_5$ across a broad range of kinetic energies compared with that obtained with a 243.1 nm probe. In phenol-$h_6$, this is not the case with the persistence of a substantial signal for low kinetic energy $H^+$, even when the probe pulse is nonresonant. The wavelength independence and broad KE distribution of this off resonance signal indicates that the origin of the $H^+$ observed (at 238 nm) in phenol-$h_6$ at low kinetic energy is very likely due to a combination of multiphoton effects such as from 238 nm alone (not observed in phenol-$d_5$) and 200 nm/238 nm, both resulting in dissociative ionization of the parent C—H bonds yielding $H^+$ directly or alternatively from the parent ion further absorbing 200 nm/238 nm light nonresonantly to yield $H^+$. Although the low kinetic energy $H^+$ observed in phenol-$h_6$ at 243.1 nm is very likely to include a
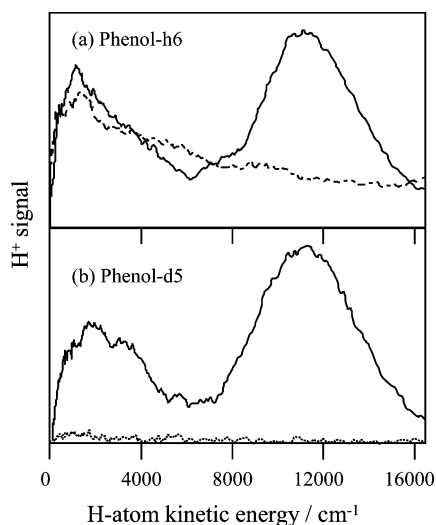
**Figure 3.** H$^+$ transient as a function of H-atom kinetic energy. Dashed and solid lines correspond to a pump (200 nm) followed by a delayed probe (2 ps) centered at 238 and 243.1 nm, respectively: (a) phenol-$h_6$ and (b) phenol-$d_5$ molecules. Note that the spectra recorded at 238 and 243.1 nm have not been normalized.



**Figure 4.** H$^+$ transients as a function of pump (200 nm)/probe (243.1 nm) delay for the low kinetic energy (a) and high kinetic energy (b) H-atoms in phenol-$d_5$. At negative time delays ($t < 0$), there is no appreciable H$^+$ signal. At positive delays, the H$^+$ signal rises sharply and plateaus beyond 500 fs. The experimental data were fitted with an exponential rise function convolved with Gaussian function of 160 fs fwhm (solid line) to yield a time constant of $146 \pm 25$ and $88 \pm 30$ fs for the slow and fast H-atoms, respectively. The error bars reported correspond to a 95% confidence limit.

significant component of H-atoms from O−H dissociation, to eliminate the ambiguity in the dynamics that arises from H$^+$ from the phenyl ring, the remaining discussion focuses on O−H fission in phenol-$d_5$.

Parts a and b of Figure 4 show the transient H$^+$ signal following photodissociation of phenol-$d_5$ at 200 and ionization at 243.1 nm. The error bars contain a confidence limit of 95%, i.e., two standard deviations of the mean. The transient H$^+$ signals were obtained by collecting a series of kinetic energy spectra at various pump/probe delays ($t$) and integrating the H$^+$

signal across discrete portions of the kinetic energy spectrum. Figure 4b corresponds to the integrated intensity obtained at the maximum of the high kinetic energy peak at 11 600 cm$^{-1}$, and Figure 4a corresponds to the integrated intensity at the low kinetic energy peak at 2700 cm$^{-1}$ (the integral widths are approximately 1000 cm$^{-1}$). In both Figure 4a,b, when the probe precedes the pump, that is, $t < 0$, no H$^+$ is observed. At $t > 0$, a sharp rise in the H$^+$ signal can be seen that plateaus at 500 fs and persists up to 2500 fs, indicative of very fast O−H bond dissociation. Fitting the time trace to a convolution of an exponential rise function with a Gaussian function (fwhm of 160 fs) yields time constants of $88 \pm 30$ and $146 \pm 25$ fs (solid black line) for the fast and slow H-atoms, respectively. For further details regarding our fitting procedure, the reader is referred to our previous work.[19]

There is a general consensus in the literature that the H-atoms with low kinetic energy must be due to some statistical decay process following population of highly excited ground-state phenol molecules.[2,8,14] However, as is clearly evident from Figure 4a, following photolysis at 200 nm, low kinetic energy H-atoms are formed on an ultrafast time scale. If these H-atoms were formed from a statistical process, we would anticipate that their appearance would be over a much longer time scale than that measured here. We have extended the delays in our pump/probe measurements to several hundred picoseconds and see no significant difference in our H$^+$ yield. We have obtained extended time H$^+$ transients for both high and low kinetic energy H-atoms showing that, even at delays approaching 200 ps, there is no identifiable increase in either transient signal, strongly indicating that there must be another, ultrafast, pathway that is giving H-atoms with the low recoil energies observed. We must note here that although a statistical pathway may still be operative, this process is likely to occur well beyond the time frame of these measurements. Indeed, we have carried out an RRKM calculation using the standard rate equation and the direct Beyer−Swinehart algorithm for vibrational density of states. We used B3LYP ab initio frequencies for phenol-$d_5$ OH at equilibrium and assumed that the three disappearing modes have half their original frequency at the transition state (S$_0$/S$_2$ CI). Using 33 000 cm$^{-1}$ as the critical energy (location of the S$_0$/S$_2$ CI) and 50 000 cm$^{-1}$ as the available energy, the RRKM calculation yielded a lifetime of the order of 65 $\mu$s. Any H-atoms formed through a statistical process will therefore represent a very small fraction of the overall yield by $t = 2$ ps. Our measured kinetic energy distributions are extremely similar to those of Nix et al. and Hause et al., obtained using nanosecond lasers, which would also be insensitive to such a slowly growing signal. Interestingly, statistical decay on S$_0$ following multiphoton excitation has a predicted time scale in the picosecond−nanosecond range, suggesting that these undesired pathways may be observed in the nanosecond experiments, but not in the present work.

Figure 5 shows the variation of the angular anisotropy parameter, $\beta_2$, as a function of kinetic energy deposited in the H fragment. We will first discuss the origins of the $\beta_2$ value for the high kinetic energy H-atoms. The positive nonlimiting $\beta_2$ value for the high kinetic energy H-atoms in the region of 12 000 cm$^{-1}$ is in clear contrast to the negative, nonlimiting $\beta_2$ for the high kinetic energy H-atoms observed by Nix et al., when pumping phenol-$h_6$ in the range 246 > $\lambda_{phot}$ > 220 nm.[23] At the excitation wavelengths described in the measurements by these authors, initial excitation accessed the S$_1$ state, where the transition dipole for the S$_1$ ← S$_0$ transition lies in a plane orthogonal to the C−O bond. Subsequent prompt dissociation leading to these fast
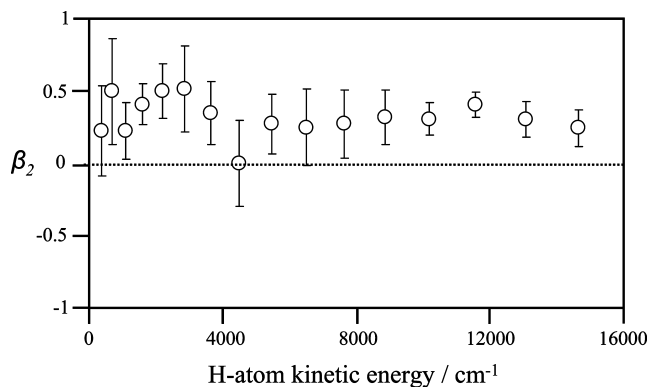
**Figure 5.** $\beta_2$ parameter as a function of kinetic energy of H fragment. The pump (200 nm)/probe (243.1 nm) delay was set at 2 ps for these measurements. At the highest kinetic energies, $\beta_2 \approx 0.4$ while at lower kinetic energies, a positive, nonlimiting $\beta_2$ still persists but with decreased signal-to-noise (see text for details).

H-atoms preserved the initial recoil anisotropy leading to a negative, nonlimiting $\beta_2 \approx -0.5$. The measurements described in this paper, however, most likely access the $S_3$ state, which is observed in the UV−vis spectrum at ∼210 nm.[2,9] From TDDFT and CASSCF[24] calculations, the $S_3$ state is predicted to be the second $^1\pi\pi^*$ where the $S_3 \leftarrow S_0$ excitation now has a transition dipole that is orthogonal to that of $S_1 \leftarrow S_0$ and is roughly aligned along the C−O bond axis. It is therefore unsurprising that following excitation to the $S_3$ state, prompt dissociation leading to H-atoms with large amounts of kinetic energy preserves the initial recoil anisotropy, leading to a *positive*, nonlimiting $\beta_2 \approx 0.4$, opposite to that observed when pumping via the $S_1$ state. Owing to the decrease in signal-to-noise at the very highest kinetic energies, it is not possible to extend these anisotropy measurements beyond 16 000 cm$^{-1}$.

For the low kinetic energy H-atoms, the anisotropy parameter still displays positive values, albeit with larger errors due to decrease in signal-to-noise. The anisotropic distribution of these low kinetic energy H-atoms is again in contrast with that observed by Nix et al. at lower photon energies in phenol-$h_6$,[23] who, in the absence of time-resolved data, assigned these fragments to single and multiphoton statistical unimolecular decay processes. The time scales involved with statistical unimolecular decay are such that any initial recoil anisotropy would be lost as the molecule would most certainly have undergone multiple rotations prior to dissociation. However, in our measurements, the time constant for the low kinetic energy H-atoms from phenol-$d_5$ is 146 ± 25 fs. Dissociation on this time scale would cause any initial recoil anisotropy to be preserved, clearly shown by Figure 5 at low kinetic energies.

Recent calculations by Vieuxmaire et al.[13] have suggested that a prefulvenic decay mechanism, similar to that observed in other single ring aromatic systems, such as benzene, may effectively compete with other decay mechanisms from the $S_1$ state, such as direct hydrogen detachment via the $^1\pi\sigma^*$ state. This interpretation has been suggested to explain the low kinetic energy H-atoms in some of the multimass ion-imaging results obtained by Tseng et al.[12] between 248 and 193 nm. The $CI_{pref}$ can provide a nonradiative decay channel resulting in the formation of highly vibrationally excited $S_0$ molecules which undergo statistical unimolecular decay. For this pathway to be effective at explaining the results in our measurements, both nonradiative population of the $S_0$ state and subsequent statistical unimolecular decay must be complete by 500 fs, as seen in Figure 4. Although this pathway may be operative at much longer time scales than in the time frame of our measurements,

it is unlikely to explain the prompt, low kinetic energy H-atoms observed here unless the majority of the excess electronic energy is deposited immediately into the O−H stretching vibrational mode for dissociation to be complete after a few vibrational periods. The calculated structure and branching space of this intersection do not indicate any role for the O−H bond extension in coupling the $S_1$ and $S_0$ states nonadiabatically, and it therefore seems unlikely that such uniquely selective internal conversion could occur at this CI.

The appearance times of these slow H-atoms (<150 fs) rules out their indirect formation through statistical unimolecular decay and we must seek an alternative explanation. Ultrashort lasers pulses are synonymous with multiphoton effects. Indeed, superexcited states populated following multiphoton excitation via $^1\pi\pi^*$ states have been shown to lead to ultrafast dynamics, via predissociation to yield H-atoms.[25] Schick and Weber have demonstrated that photoelectrons generated by autoionisation of these superexcited states, following multiphoton excitation around the ionization potential of phenol (8.5 eV),[26] occur with appearance times shorter than their instrumental response function (<230 fs),[25] suggesting that the decay lifetimes of these excited states into the ionization continuum is equally prompt. Two-photon excitation with 200 nm light used here would result in excitation well-above the ionization potential of phenol, increasing the autoionisation rate and limiting the role of superexcited states in producing neutral H atoms via a predissociation mechanism occurring with a ∼150 fs time scale. It therefore seems unlikely that these states explain the low kinetic energy H-atom appearance times that have been measured here.

Recent measurements by Devine et al. in thiophenol[27] have shown that, following excitation above the $S_1/S_2$ CI, both the ground and electronically excited phenylthiyl radicals ($C_6H_5S$, X- and A-state, respectively) were formed. The fastest H-atoms resulting from the X-state $C_6H_5S$ showed a recoil anisotropy of $\beta_2 \approx -0.45$, whereas the slower H-atoms appeared more isotropic. While the $\beta_2$ associated with the fastest H-atoms corresponding to A-state $C_6H_5S$ was also expected to give a negative $\beta_2$, the larger isotropic contribution from highly excited X-state $C_6H_5S$ fragments with the same total kinetic energy washed out any anisotropy.

The persistence of a positive, nonlimiting $\beta_2$ at low kinetic energies can also be explained on the basis that in our measurements on phenol-$d_5$, both ground and electronically excited phenoxyl-$d_5$ radicals ($C_6D_5O$) are formed. As in thiophenol, A-state $C_6D_5O$ is also expected to give a partially positive $\beta_2$, subject to masking by any isotropic contribution from highly excited X-state $C_6D_5O$ with the same total kinetic energy (which could also explain the increased error bars). Interestingly, the A-state of $C_6H_5O$ lies ∼8900 cm$^{-1}$ above the ground state as compared to the A-state of $C_6H_5S$ ∼2800 cm$^{-1}$. Therefore, given that branching to the A-state asymptote is expected to occur at the $S_0/S_2$ CI, we would expect the X- and A-state products to be formed with similar internal excitation, determined much nearer the Franck−Condon region. This would lead one to expect A-state products to peak at ∼2700 cm$^{-1}$ (11 600−8900 cm$^{-1}$), in good agreement with the observed peak center (clearly displayed by the lower kinetic energy peak in Figure 5). As a result of the increased A ← X separation in phenol relative to thiophenol, the $S_0/S_2$ CI in phenol occurs at a much shorter $R_{X-H}$ bond distance. This results in a much steeper gradient at the CI in phenol. This will most likely result in a lower probability for the adiabatic dynamics at the $S_0/S_2$ CI in phenol-$d_5$ that would ultimately lead to excited phenoxyl-$d_5$ fragments, reducing the propensity for excited-state products, which could

explain the observed peak intensity ratio between the low and high kinetic energy H-atoms shown in Figure 2b.

Further evidence that the low kinetic energy component of the spectrum is due to A-state phenoxyl-$d_5$ comes from measuring different time scales of dissociation for the low and high kinetic energy components. As shown in Figure 4a,b, the $H^+$ transients clearly show two different time constants of 146 $\pm$ 25 and 88 $\pm$ 30 fs (solid black line) for the slow and fast H-atoms, respectively. The different time scales can once again be rationalized on the basis of the competing adiabatic vs nonadiabatic dynamics at the $S_0/S_2$ CI. For dissociation to occur adiabatically and yield electronically excited phenoxyl-$d_5$ fragments, the wavepacket will undoubtedly decelerate as it avoids the CI and begins climbing up the potential energy surface to dissociate adiabatically at the A-state asymptote. This simple classical picture can be used to rationalize the factor of $\sim$2 difference in time scales observed. Indeed, a factor of 4 difference in the kinetic energies of the two exit channels translates to a factor of 2 difference in the velocities and hence the time scales, in very good agreement with the measured value. Both models support the rationale that A-state phenoxyl-$d_5$ fragments are responsible for the low kinetic energy H-atoms which, owing to their direct nature, display positive, nonlimiting $\beta_2$.

It is important to mention that, recently, while exciting phenol-$d_5$ molecules at 193 nm, TKER measurements by Ashfold et al.[28] have revealed another pathway for H-atom elimination, not observed in their previous measurements at 206 nm. This channel yields a structured signal at $\sim$5500 cm$^{-1}$ in the TKER spectrum and is attributed to the formation of vibrationally cold $C_6D_5O$ cofragments in their second excited state (B-state). This suggests the existence of another CI at extended $R_{O-H}$ at an excitation energy of $\sim$6.4 eV providing a route from the optically bright $S_3$ state to another higher $^1\pi\sigma^*$ state, which correlates with the phenoxyl B-state. CASPT2 calculations in the same work revealed that the onset of this channel occurs at $\sim$6.4 eV, where the $S_3$ and upper $^1\pi\sigma^*$ states intersect. In our measurements while pumping phenol-$d_5$ molecules at 200 nm ($\sim$6.2 eV), if we assume that this channel is accessible by tunnelling, internally cold $C_6D_5O$ fragments in their B-state would result in a peak at $\sim$4000 cm$^{-1}$. While the relatively poor resolution of our VMI spectrometer, in comparison to the H Rydberg atom photofragment translational spectroscopy method and the threshold nature of this channel at 200 nm prohibits clear identification of this channel, it must result in at most a minor contribution to the low kinetic energy signal at 200 nm. It seems most likely that the threshold energy for the $S_3/^1\pi\sigma^*$ CI has not been achieved and the channel remains closed.

## Conclusions

The competition between statistical vs nonstatistical deactivation pathways in heteroaromatics has been a subject of increasing interest in the very recent literature. One of the contributing factors that has fuelled such curiosity is the presence of optically dark $^1\pi\sigma^*$ states. The $^1\pi\sigma^*$ states are dissociative along the X$-$H coordinate, where X is typically N or O, leading to H-atoms with high kinetic energies. However, additional low kinetic energy H atoms are often released in these photolysis experiments. Using a combination of femtosecond pump/probe spectroscopy and VMI, we have been able to clock the real-time dissociation of the O$-$H bond in phenol-$d_5$, following excitation of the optically bright $S_3$ state at 200 nm. From these measurements, we infer that the direct H-atoms with high kinetic energies form with a time-constant of 88 $\pm$ 30 fs, in a

nonstatistical decay route involving passage through or around three successive CIs ($S_1/S_3$, $S_1/S_2$, and $S_0/S_2$) to form H + $C_6D_5O$ in its electronic ground state. The H-atoms with lower kinetic energy, rising with a time-constant of 146 $\pm$ 25 fs also appear to form via a nonstatistical decay route, involving the same decay pathway, but leading to electronically excited phenoxyl-$d_5$ radicals due to branching induced by adiabatic dynamics in the region of the final ($S_0/S_2$) CI. Whether these slow H-atoms are a result of the phenoxyl cofragment being formed electronically excited, or are due to multiphoton processes and superexcited states, is still open to debate. We favor the former interpretation given previous work on thiophenol, the known term value for the A $\leftarrow$ X transition in phenoxyl and the anisotropy measurements. Nonlimiting, positive $\beta_2$ for low kinetic energy H-atoms bring into question the presence of indirect dynamics, thus ruling out the possibility of these H atoms being associated with single photon unimolecular decay leading to hot ground-state phenoxyl radicals. The appearance of these H atoms at a time scale of 146 fs also suggests direct dynamics prevail, ruling out a statistical pathway for the O$-$H bond fission. It is still possible that ring D-atoms may dissociate statistically although the similarity of our phenol-$d_5$ and phenol-$h_6$ data leads us to suspect this channel is at most a minor one.

Multiphoton processes, mediated by superexcited states may be operative given the pump wavelengths used here (200 nm), although multiphoton absorption will lead to excitation wellabove the ionization potential, increasing the autoionisation rate and reducing the likelihood of direct dynamics from these states. Furthermore, one might expect extremely high kinetic energy release following photoexcitation to these neutral states (25 000 cm$^{-1}$),[29] in contrast to the observed low kinetic energy release associated with the 146 fs channel.

While these measurements illustrate the need for further highlevel calculations, what is clearly evident from this work on phenol-$d_5$ is the appearance of low kinetic energy H-atoms, which might previously have been attributed to some single photon statistical pathway, should be interpreted in terms of direct processes, most likely leading to excited-state phenoxyl-$d_5$ products. In fully hydrogenated systems, the low kinetic energy $H^+$ signals are often enhanced and take on a typical "statistical decay" kinetic energy profile. It seems likely that these signals are multicomponent and comprise multiphoton statistical decay, which may occur with a rather longer time constant, in addition to "direct channels" leading to excitedstate products. The combination of time and energy resolved VMI with selective deuteration of the aromatic ring has made it possible to disentangle these contributions in phenol-$d_5$ and confirm the direct dynamical nature of the low kinetic energy channel in $C_6D_5OH$ photolysis at 200 nm.

## References and Notes

(1) Sobolewski, A. L.; Domcke, W. *Chem. Phys.* **2000**, *259*, 181.
(2) Ashfold, M. N. R.; Cronin, B.; Devine, A. L.; Dixon, R. N.; Nix, M. G. D. *Science* **2006**, *312*, 1637.
(3) Callis, P. R. *Annu. Rev. Phys. Chem.* **1983**, *34*, 329.

(4) Creed, D. *Photochem. Photobiol.* **1984**, *39*, 537.

(5) Sobolewski, A. L.; Domcke, W. *J. Phys. Chem. A* **2001**, *105*, 9275.

(6) Sobolewski, A. L.; Domcke, W.; Dedonder-Lardeux, C.; Jouvet, C. *Phys. Chem. Chem. Phys.* **2002**, *4*, 1093.

(7) Lan, Z.; Domcke, W.; Vallet, V.; Sobolewski, A. L.; Mahapatra, S. *J. Chem. Phys.* **2005**, *122*, 224315.

(8) Ashfold, M. N. R.; Devine, A. L.; Dixon, R. N.; King, G. A.; Nix, M. G. D.; Oliver, T. A. A. *Proc. Natl. Acad. Sci. U.S.A.* **2008**, *105*, 12701.

(9) Kimura, K.; Nagakura, S. *Mol. Phys.* **1965**, *9*, 117.

(10) Tseng, C. M.; Lee, Y. T.; Ni, C. K. *J. Chem. Phys.* **2004**, *121*, 2459.

(11) Tseng, C. M.; Lee, Y. T.; Ni, C. K.; Chang, J. L. *J. Phys. Chem. A* **2007**, *111*, 6674.

(12) Tseng, C. M.; Lee, Y. T.; Lin, M. F.; Ni, C. K.; Liu, S. Y.; Lee, Y. P.; Xu, Z. F.; Lin, M. C. *J. Phys. Chem. A* **2007**, *111*, 9463.

(13) Vieuxmaire, O. P. J.; Lan, Z.; Sobolewski, A. L.; Domcke, W. *J. Chem. Phys.* **2008**, *129*, 224307.

(14) Hause, M. L.; Yoon, Y. H.; Case, A. S.; Crim, F. F. *J. Chem. Phys.* **2008**, *128*, 104307.

(15) Lucas, B.; Barat, M.; Fayeton, J. A.; Jouvet, C.; Carçabal, P. *Chem. Phys.* **2008**, *347*, 324.

(16) Grégoire, G.; Kang, H.; Dedonder-Lardeux, C.; Jouvet, C.; Desfrançois, C.; Onidas, D.; Lepere, V.; Fayeton, J. A. *Phys. Chem. Chem. Phys.* **2006**, *8*, 122.

(17) Lippert, H.; Ritze, H.-H.; Hertel, I. V.; Radloff, W. *ChemPhysChem.* **2004**, *5*, 1423.

(18) Iqbal, A.; Pegg, L.-J.; Stavros, V. G. *J. Phys. Chem. A* **2008**, *112*, 9531.

(19) Wells, K. L.; Perriam, G.; Stavros, V. G. *J. Chem. Phys.* **2009**, *130*, 074308.

(20) Even, U.; Jortner, J.; Noy, D.; Lavie, N.; Cossart-Magos, C. *J. Chem. Phys.* **2000**, *112*, 8068.

(21) Eppink, A. T. J. B.; Parker, D. H. *Rev. Sci. Instrum.* **1997**, *68*, 3477.

(22) Roberts, G. M.; Nixon, J. L.; Lecointre, J.; Wrede, E.; Verlet, J. R. R. *Rev. Sci. Instrum.* **2009**, *80*, 053104.

(23) Nix, M. G. D.; Devine, A. L.; Cronin, B.; Dixon, R. N.; Ashfold, M. N. R. *J. Chem. Phys.* **2006**, *125*, 133318.

(24) Frisch, M. J.; Trucks, G. W.; Schlegel, H. B.; Scuseria, G. E.; Robb, M. A.; Cheeseman, J. R.; Montgomery, J. A., Jr.; Vreven, T.; Kudin, K. N.; Burant, J. C.; Millam, J. M.; Iyengar, S. S.; Tomasi, J.; Barone, V.; Mennucci, B.; Cossi, M.; Scalmani, G.; Rega, N.; Petersson, G. A.; Nakatsuji, H.; Hada, M.; Ehara, M.; Toyota, K.; Fukuda, R.; Hasegawa, J.; Ishida, M.; Nakajima, T.; Honda, Y.; Kitao, O.; Nakai, H.; Klene, M.; Li, X.; Knox, J. E.; Hratchian, H. P.; Cross, J. B.; Bakken, V.; Adamo, C.; Jaramillo, J.; Gomperts, R.; Stratmann, R. E.; Yazyev, O.; Austin, A. J.; Cammi, R.; Pomelli, C.; Ochterski, J. W.; Ayala, P. Y.; Morokuma, K.; Voth, G. A.; Salvador, P.; Dannenberg, J. J.; Zakrzewski, V. G.; Dapprich, S.; Daniels, A. D.; Strain, M. C.; Farkas, O.; Malick, D. K.; Rabuck, A. D.; Raghavachari, K.; Foresman, J. B.; Ortiz, J. V.; Cui, Q.; Baboul, A. G.; Clifford, S.; Cioslowski, J.; Stefanov, B. B.; Liu, G.; Liashenko, A.; Piskorz, P.; Komaromi, I.; Martin, R. L.; Fox, D. J.; Keith, T.; Al-Laham, M. A.; Peng, C. Y.; Nanayakkara, A.; Challacombe, M.; Gill, P. M. W.; Johnson, B.; Chen, W.; Wong, M. W.; Gonzalez, C.; Pople, J. A. *Gaussian 03*, revision B.04; Gaussian, Inc.: Pittsburgh, PA, 2003.

(25) Schick, C. P.; Weber, P. M. *J. Phys. Chem. A* **2001**, *105*, 3725.

(26) Lipert, R. J.; Colson, S. D. *J. Chem. Phys.* **1990**, *92*, 3240.

(27) Devine, A. L.; Nix, M. G. D.; Dixon, R. N.; Ashfold, M. N. R. *J. Phys. Chem. A* **2008**, *112*, 9563.

(28) King, G. A.; Oliver, T. A. A.; Nix, M. G. D.; Ashfold, M. N. R. *J. Phys. Chem. A*, published online June 18, http://dx.doi.org/10.1021/jp9031404.

(29) Devine, A. L.; Nix, M. G. D.; Cronin, B.; Ashfold, M. N. R. *Phys. Chem. Chem. Phys.* **2007**, *9*, 3749.